

Room-temperature Coulomb staircase in semiconducting InP nanowires modulated with light illumination

[Nanotechnology 22 (5), 055201 (2011)]

Toshishige Yamada^{*a),b)}, Hidenori Yamada^{c)}, Andrew J. Lohn^{b),d)}, and Nobuhiko P. Kobayashi^{b),d)}

^{a)}*Center for Nanostructures, School of Engineering, Santa Clara University, Santa Clara, California 95053*

^{b)}*Department of Electrical Engineering, Baskin School of Engineering, University of California, Santa Cruz, Santa Cruz, California 95064*

^{c)}*Department of Electrical Engineering and Computer Sciences, University of California, Berkeley, Berkeley, California 94720*

^{d)}*Nanostructured Energy Conversion Technology and Research (NECTAR), Advanced Studies Laboratories, University of California Santa Cruz and NASA Ames Research Center, Moffett Field, California 94035*

*Author to whom correspondence should be addressed: tyamada@scu.edu.

Abstract: Detailed electron transport analysis is performed for an ensemble of conical indium phosphide nanowires bridging two hydrogenated n^+ -silicon electrodes. The current-voltage (I - V) characteristics exhibit a Coulomb staircase in dark with a period of ~ 1 V at room temperature. The staircase is found to disappear under light illumination. This observation can be explained by assuming the presence of a tiny Coulomb island, and its existence is possible due to the large surface depletion region created within contributing nanowires. Electrons tunnel in and out of the Coulomb island, resulting in the Coulomb staircase I - V . Applying light illumination raises the electron quasi-Fermi level and the tunneling barriers are buried, causing the Coulomb staircase to disappear.

PACS: 73.23.Hk, 78.67.-n, 85.35.-p, 68.47.Fg

Key words: InP, semiconducting nanowire, Coulomb staircase, illumination

INTRODUCTION

Indium phosphide nanowires (InP NWs) attract a lot of attention [1]. Kobayashi et al. reported In NW synthesis and electrical transport measurements on a simple photoconductor under light illumination [2]. On their photoconductor with two hydrogenated Si (Si:H) electrodes, InP was grown into cone-shaped nanowires with bases attached on the electrodes as shown in figures 1(a) and 1(b). Some of the NWs encountered each other during the growth and fused together in pairs as in figure 1(c), establishing an electrical connection. Since the Si:H electrodes were n^+ -doped and InP was unintentionally n -doped regardless of synthesis methods [3], electrons dominantly contributed to electrical transport. In this paper, we describe detailed analysis on the DC electron transport characteristics of the InP NW photoconductor in dark and under light illumination with monochromatic light (633 nm, 1.95 eV) at various optical power levels ranging up to 5 μ W. The light energy is well beyond the InP direct band gap E_g of 1.34 eV so that appreciable electron-hole (e-h) pair generation is expected. One electrode (drain) was biased at $V_d = -5$ to 5 V while the other (source) was grounded, and the current I_d flowing into and out of these electrodes was measured. It has to be emphasized that all data were taken at room temperature.

We have examined several devices, and have observed increasing photoconductor conductance as the illumination power is increased due to the e-h generation. Nearly a half of the devices showed a smooth I_d - V_d curve in dark with a slight diverging nonlinearity ($d^2I_d/dV_d^2 > 0$ when $V_d > 0$, or $d^2I_d/dV_d^2 < 0$ when $V_d < 0$) and the NW differential conductance between the electrodes $R_{NW} = dI_d/dV_d$ changed from ~ 2 nS at $V_d = 0$ to ~ 5 nS at $V_d = 5$ V. The illumination increased the device photoconductivity by orders of magnitude, which is quite important in the engineering context, but everything was well understood in the

physics context. The details are discussed regarding figure 3 of Ref. 4. However, the remaining devices showed an unusual I_d - V_d behavior in dark as detailed below and it gradually disappeared under illumination. The present article focuses on the behavior of these devices.

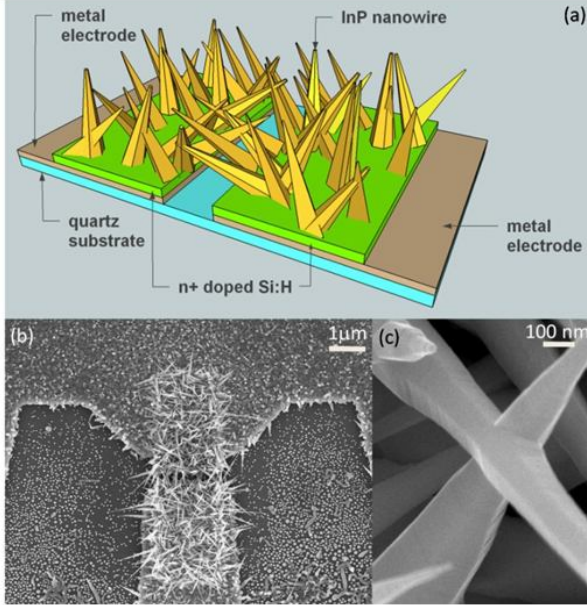


Figure 1. (a) Schematic of a fabricated InP nanowire (NW) photoconductor. (b) Scanning electron microscope (SEM) image (top view) of a representative InP NW photoconductor. InP NWs were selectively grown on the pair of n^+ -doped Si:H electrodes. (c) SEM image of a point where two nanowires were fused.

STAIRCASE CURRENT-VOLTAGE CHARACTERISTICS

The resulting plot of I_d vs. V_d is shown in figure 2(a) with light illumination power indicated in μW under which a specific I_d - V_d curve is collected. The photoconductor conductance increases approximately $0.06 \mu\text{S}$ with each μW increment of power, and reaches an order of magnitude higher value at $5 \mu\text{W}$. As clearly seen in figure 2(a), there are substantial differences in the I_d - V_d curve in dark compared to those under light illumination. I_d increases discretely with V_d , demonstrating evident periodic staircase characteristics in dark. To extract the staircase period ΔV in dark, we have subtracted the linear component of the current, and then performed Fourier transform as in figure 2(b). The peak is reached at $2\pi/\Delta V = 6.6 \text{ V}^{-1}$ or $\Delta V = 0.95 \text{ V}$. We have also examined the data by plotting d^2I_d/dV_d^2 and performing Fourier transformation, which led us to practically identical results. Under light illumination at $0.64 \mu\text{W}$, the weak wavy characteristics associated with the periodic staircase still remain with smaller ΔV while the linear component is noticeably large. However, the NW photoconductor shows Ohmic characteristics under light illumination at $1.1 \mu\text{W}$ and higher: I_d increases smoothly as V_d increases and the staircase disappears. These changes are reversible, *i.e.*, the I_d - V_d characteristics in dark are identical even after going through progressive illumination cycles. Devices with the staircase in dark exhibit $dI_d/dV_d \sim I_d/V_d \sim 10 \text{ nS}$, (I_d - V_d is linear if neglecting the staircase fine structure), while those without the staircase exhibit $dI_d/dV_d \sim 2 \text{ nS}$ at $V_d = 0$ and $\sim 5 \text{ nS}$ at $V_d = 5 \text{ V}$.

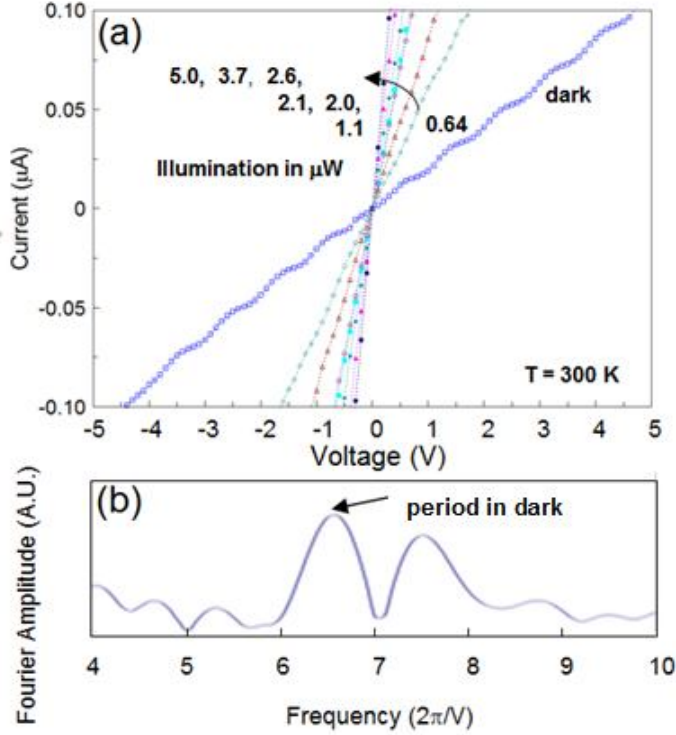


Figure 2. (a) I_d as a function of V_d with light power as a parameter. (b) Fourier transform of $I_d(V_d) - cV_d$, where c is a constant. The peak is at $2\pi/V = 6.6 \text{ V}^{-1}$, corresponding to the staircase period of $\Delta V = 0.95 \text{ V}$.

The I_d - V_d characteristics collected in dark are reminiscent of a Coulomb staircase [5-13], which is typical for a structure of "conductor – tunneling barrier (capacitor) – Coulomb island – tunneling barrier (capacitor) – conductor" as shown in figure 3(a) inset. We here use thermodynamics and describe the Coulomb staircase in a more intuitive way [8-13]. Two conditions must be satisfied: (i) the Coulomb charging energy is much larger than the ambient thermal energy $k_B T$; (ii) tunneling resistance R_T is much larger than quantum resistance of $R_Q = h/2q^2 = 12.9 \text{ k}\Omega$, with h the Planck constant and q the unit charge. Generally, the minimum internal energy and maximum entropy requirements conflict and thus we usually minimize the free energy $F(N) = U(N) - TS$ at given temperature T , where $U(N)$ is the internal energy when the island has N electrons and S is the entropy. However, because of condition (i), the internal energy U is dominant in F (or $F \sim U$) and the minimization of U will explain the essential physics. We consider a capacitance circuit as in the inset of figure 3 with the source capacitor C_s grounded ($V_s = 0$), the drain capacitor C_d biased at V_d , and the gate capacitor C_g biased at V_g . The gate electrode with a C_g is included for better description of thermodynamics even though it is absent in our experiment (we can take a limit of $C_g \rightarrow 0$ and $V_g \rightarrow 0$ with no tunneling possibility from/to the gate electrode). The change ΔU is evaluated for an incoming electron tunneling event from electrode k ($k = s$ or d) to the island, where the number of electrons changes from $N-1$ to N . Because of condition (ii), electrons are isolated on the island and their numbers are quantized [14]. The island gains the coulomb energy by $U_C(N) - U_C(N-1)$, where $U_C(N) = (Nq)^2/2C$ and $C = C_s + C_d + C_g$ is the island capacitance. The potential energy also changes with this tunneling because electrode k loses $-|q|V_k$ and the island gains $-|q|V_{\text{island}}$, where $V_{\text{island}} = (C_d V_d + C_g V_g)/C$ is an island voltage. The resultant ΔU is therefore given by

$$\Delta U(N,k) = U_C(N) - U_C(N-1) - |q|(C_d V_d + C_g V_g)/C + |q|V_k . \quad (1)$$

By introducing new variables

$$E_N = U_C(N) - U_C(N-1) - |q|(C_d V_d + C_g V_g)/C, \quad (2)$$

$$E_k = -|q|V_k, \quad (3)$$

we have

$$\Delta U(N,s) = E_N - E_s = E_N, \quad (4)$$

$$\Delta U(N,d) = E_N - E_d. \quad (5)$$

The rules guiding tunneling are as follows:

- (i) If $\Delta U(N,k) = E_N - E_k < 0$, an electron tunnels *in* from electrode k to the island with N *final* electrons (the island electrons change from $N-1$ to N).
- (ii) If $\Delta U(N,k) = E_N - E_k > 0$, an electron tunnels *out* from the island with N *initial* electrons to electrode k (the island electrons change from N to $N-1$).

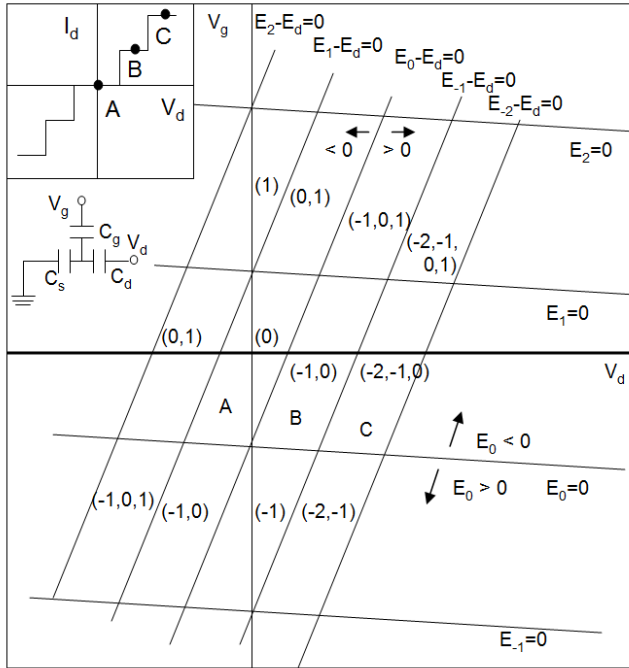


Figure 3. Internal energy change $\Delta(N,k) = E_N - E_k$ after incoming electron tunneling to the island from electrode k in the V_g - V_d plane. If $E_N - E_k < 0$, an electron tunnels *in* from electrode k to the island with N *final* electrons (the island electrons change from $N-1$ to N). If $E_N - E_k > 0$, an electron tunnels *out* from the island with N *initial* electrons to electrode k (the island electrons change from N to $N-1$).

Figure 3 is a diagram for how E_N and $E_N - E_d$ change in the V_g - V_d plane, where the V_d axis ($V_g = 0$) is our interest. Considering our staircase characteristics with a clear period, it is assumed that the pair of tunneling capacitances are asymmetric, i.e., $C_d \ll C_s$. In fact, otherwise, lines for $E_N = 0$ will have an appreciable negative slope and intersect with the V_d axis, resulting in the disturbed staircase period.

Depending on V_d , there are parallelogram regions corresponding to each step of the staircase, A, B, and C, in figure 3. The signs of E_N and $E_N - E_d$ are listed in figures 4(a)-4(c) and the evolution of N is indicated, respectively.

In region A in figure 4(a), when $N \leq -1$, $E_N < 0$ and $E_N - E_d < 0$ and this means when the island has -1 electron or less (larger negative numbers), incoming tunneling of an electron from the source or drain occurs until the island has zero electrons. When $N \geq 0$, $E_N > 0$ and $E_N - E_d > 0$ and this means when the island has $+1$ electron or more, outgoing tunneling of an electron to the source or drain occurs until the island has zero electrons. Thus, zero drain current flows in the steady state with $N = 1$.

In region B in figure 4(b), the source shows the same behavior as that in region A. However, the drain shows a different behavior due to increased $V_d > 0$, i.e., when $N \leq 0$, $E_N - E_d < 0$, and $N \geq 1$, $E_N - E_d > 0$. Thus, the island can take $N = -1$ or 0 . Suppose $N = -1$. An electron tunnels *in* from the *source* because $E_0 < 0$ while incoming tunneling from the drain is forbidden because $E_0 - E_d > 0$, and then $N = 0$. The same electron tunnels *out* to the *drain* because $E_0 - E_d > 0$ while outgoing tunneling to the source is forbidden because $E_0 < 0$, and then $N = -1$. This completes one cycle. In this process, current carried by a *single* electron flows from the drain to source.

In region C in figure 4(c), the source shows the same behavior as that in regions A and B. However, the drain shows a further different behavior due to further increased $V_d > 0$, i.e., when $N \leq 0$, $E_N - E_d < 0$, and $N \geq 1$, $E_N - E_d > 0$. Thus, the island can take $N = -2$, -1 , or 0 . Suppose $N = -2$. An electron tunnels *in* from the *source* because $E_{-1} < 0$ while outgoing tunneling from the drain is forbidden because $E_{-1} - E_d < 0$, and then $N = -1$. Another electron tunnels *in* from the *source* successively because $E_0 < 0$ while outgoing tunneling to the source is forbidden because $E_{-1} - E_d > 0$, and then $N = 0$. Then, one of these two electrons tunnels *out* to the *drain* because $E_0 - E_d > 0$ while outgoing tunneling to the source is forbidden because $E_0 < 0$, and then $N = -1$. The remaining electron tunnels *out* to the *drain* because $E_{-1} - E_d > 0$ while outgoing tunneling to the source is forbidden because $E_{-1} < 0$, and then $N = -2$. This completes one cycle. The current carried by *two* electrons flows from the drain to source.

If we assume it takes almost the same time τ to complete each cycle, then drain current is 0 for region A, $|q|/\tau$ for region B, and $2|q|/\tau$ for region C, etc.

Tunneling barriers will act as tunneling capacitors in the equivalent circuit picture. When this structure is embedded in our system of Si:H electrode – fused InP NW – Si:H electrode, the Coulomb staircase will be observed if (i) the Coulomb charging energy is much larger than the ambient thermal energy $k_B T$, and (ii) tunneling resistance R_T is much larger than quantum resistance of $R_Q = h/2q^2 = 12.9$ k Ω , so that the island is isolated and can accommodate an integer number of electrons [13,14]. Then, spatially correlated successive tunneling of an electron from source to drain occurs and the Coulomb staircase results [8-13]. Our analysis below strongly suggests that the Coulomb staircase is exhibited at room temperature.

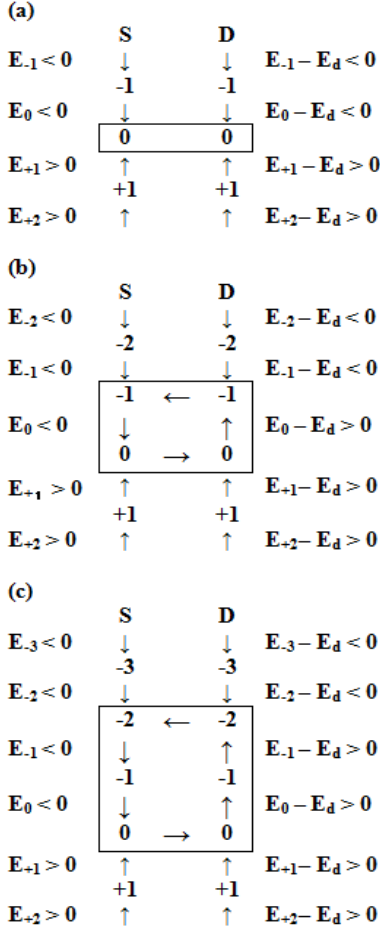


Figure 4. Evolution in the number of electrons on the island for different bias V_d . (a) region A of zero current, with the number of thermodynamically allowed island electrons (N) is 0, (b) region B of unit current with $N = -1$ and 0, and (c) region C of two units of current with $N = -2, -1$, and 0. Arrows indicate how tunneling occurs and N changes.

ANALYSIS OF EXPERIMENT

We first examine the influence of illumination to the staircase qualitatively. In dark, the Fermi level E_{F0} is well below the two tunneling barriers corresponding to capacitors C_s and C_d . When an electron tunnels to the island, the charging energy is $\sim q^2/C_\Sigma$, where $C_\Sigma = C_s + C_d$. The charging energy is comparable to $q\Delta V = 0.95$ eV and is much larger than $k_B T = 26$ meV. The total resistance R_{tot} reflecting R_T is in the 10 M Ω range, much larger than $R_Q = 12.9$ k Ω . Therefore, the staircase I_d - V_d characteristics are seen in dark [8-13]. Under light illumination, a lot of e-h pairs are generated and E_{F0} splits into quasi-Fermi levels for electrons E_{Fn} and holes E_{Fp} . E_{Fn} will rise as the light illumination power P is increased, from E_{F0} to E_{Fn1} in the schematic energy diagram of figure 5(a) inset. ΔV decreases at $P = 0.64$ μ W compared to that in dark, and this is consistent with decreasing $1/C_s$ and $1/C_d$ (due to the effective reduction of the capacitor-plate distance) with rising E_{Fn} with P . When E_{Fn} rises to E_{Fn2} , the tunneling barriers are mostly located below it and these capacitors practically disappear ($1/C_s$ and $1/C_d \rightarrow 0$). As a result, the system can be regarded as a simple resistor, and linear I_d - V_d characteristics result with a much lower resistance. This scenario is all consistent with our experimental observations. In the following, we will analyze the experimental data quantitatively, and show that this scenario is in fact a conceivable explanation for our unique NW photoconductor behavior in dark and under light illumination.

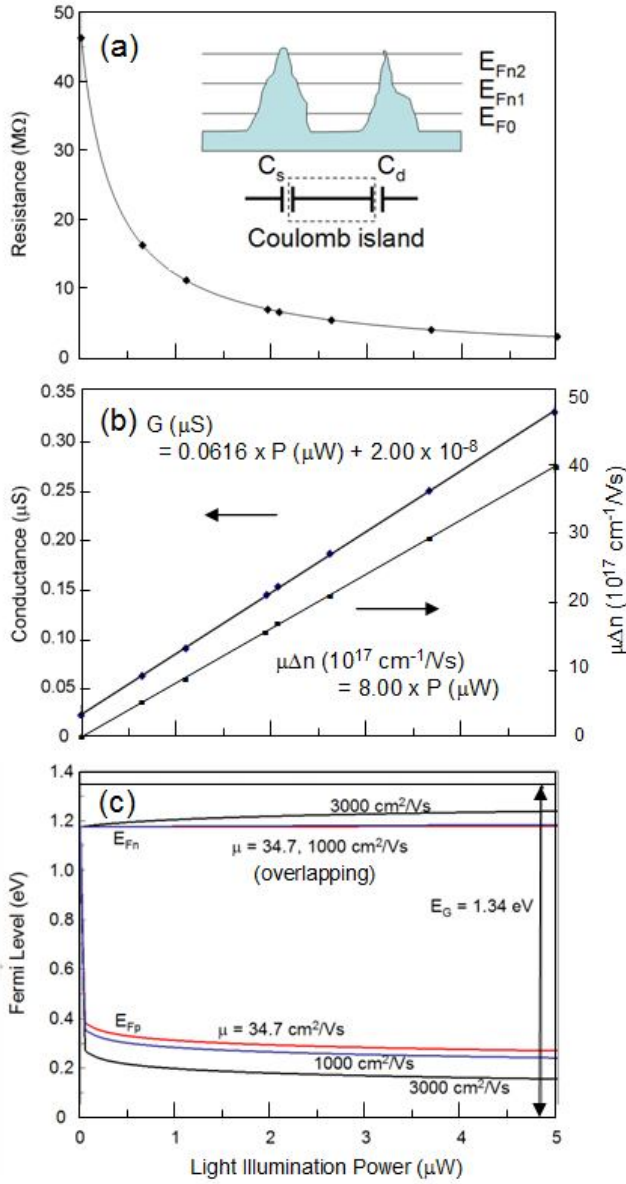


Figure 5. (a) Resistance R_{tot} as a function of light illumination power P , where each dot represents a measured point. Inset: Schematic energy band diagrams for a Coulomb island and barriers for Fermi levels E_{F0} , E_{F1} , and E_{F2} . (b) Conductance G and $\mu\Delta n$ as a function of P . (c) E_{Fn} and E_{Fp} as a function of P for representative electron mobility μ values, 34.7 [17], 1000, and 3000 cm²/Vs.

The model assumes a *single* active Coulomb island on a pair of NWs while our structural analysis (figure 1) clearly shows multiple fused NW pairs bridging two electrodes (we have identified twelve NW pairs on average present per photoconductor) [1]. Since these NW pairs are connected to Si:H electrodes in parallel, the assumption is equivalent to that one pair has resistance substantially lower than the other pairs, and determines overall I_d - V_d characteristics. This is a legitimate assertion since R_T through the above barriers will be an important source in resistance. In fact, tunneling transport is widely seen in various nanoscale systems, and R_T depends on the tunnel barrier width exponentially. As a result, R_T can change by an order of magnitude even with a very small atomic scale change of ~ 0.1 nm in tunneling

barrier width [15]. Since microscopic details of the multiple fused NW pairs are all different, there would be appreciable variations in tunneling barrier among the NW pairs, resulting in significant difference (orders of magnitude) in R_T .

To further extend the view, two tunneling barriers are also highly likely to be asymmetric, and the tunneling resistance for one barrier can be an order of magnitude different from that for the other. In this case the barrier with less tunneling dominates transport, and the staircase period ΔV is q/C_i , where C_i is the dominant barrier capacitance ($i = s$ or d) [5]. From figure 2(b), $\Delta V = 0.95$ V and this suggests the presence of very small capacitances in the range of 0.1 aF in a NW pair. C_i can be given by $C_i = \alpha \times \epsilon A/d$ even when the plate area A and the distance squared d^2 are comparable, where α is a dimensionless factor ($\sim 10^0$) representing the capacitance fringing field effects [16]. Using this expression, we estimate that the physical dimension of these capacitors is a rectangular prism of $A = 10$ nm² and $d \sim 0.5$ nm with a vacuum dielectric constant $\epsilon \sim 1$ (the tunneling barrier corresponding to a vacuum gap in the InP background). In some devices, the staircase characteristics are not observed, and this is interpreted that the necessary pair of capacitors are not successfully formed, resulting in the staircaseless smooth I_d - V_d characteristics.

These capacitors are significantly smaller than the typical NW radius of ~ 0.1 μm around the fused portion. However, the fact that InP NWs are unintentionally doped semiconductors and their surfaces are largely depleted suggests that it is not the physical dimension of the fused portion that accounts for the capacitance. Unintentionally doped InP thin films synthesized by metal-organic chemical vapor deposition are usually n -type with the electron density of $n \sim 10^{15}$ cm⁻³, while unintentionally doped InP thin films grown by molecular beam epitaxy (MBE) *from solid sources* are consistently n -type with $n \sim 10^{16}$ cm⁻³ (in exceptional cases, $n \sim 5 \times 10^{14}$ to 5×10^{15} cm⁻³ is reported in MBE grown InP) [2]. We have confirmed that our unintentionally doped InP blanket films are n -type with $n \sim 10^{15}$ cm⁻³. This means that our significantly wide NWs can have $n \sim 10^{15}$ cm⁻³, but our narrow NWs could have up to $n \sim 10^{16}$ cm⁻³. The depletion region width w_{dep} is estimated with the abrupt planar junction formula $(2\epsilon V_{\text{surf}}/qn)^{1/2}$ using the depletion approximation [17], where ϵ is an InP dielectric constant 12.5 with respect to that of vacuum, V_{surf} is a surface potential. Assuming $V_{\text{surf}} \sim 0.1$ eV (V_{surf} is a fraction of E_g [18]), we estimate $w_{\text{dep}} \sim 0.3$ μm for $n = 10^{15}$ cm⁻³, and $w_{\text{dep}} \sim 0.1$ μm for $n = 10^{16}$ cm⁻³. The staircase scenario demands that the radius and w_{dep} be comparable near the fused portion of cone-shaped NWs whose radius be ~ 0.1 μm [19] and there be an active conducting region near the NW central axis. If we consider there would be a possibility of systematic increased doping (thermodynamic or kinetic), e.g., $n \sim 10^{16}$ cm⁻³ towards the tip of the NWs, everything is consistent with our proposed mechanisms to explain the experimental observations: NW devices are electrically conducting even though NWs are connected via fused portions of ~ 0.1 μm and ~ 10 nm² \times 0.5 nm rectangular prism capacitors exist near the Coulomb island deep inside the NWs.

Because of large w_{dep} , it would be highly possible that capacitances of ~ 10 nm² \times 0.5 nm rectangular prisms are present within much wider NWs. In fact, this is an important and substantial difference between metallic and semiconducting nanostructures. In metals, $w_{\text{dep}} \sim 0$ due to large n , and once the capacitor physical size is estimated in modeling, identifying the capacitor location would be straightforward. After capacitor size estimation, Hanna and Tinkham suggested that capacitors should be located between the scanning tunneling microscope (STM) tip and metallic sample, and proved it through their observation of I_d - V_d modulation when changing the STM-sample distance [5]. Matsumoto *et al.* created a surrounding barrier and a resultant metallic Coulomb island with pre-designed dimension by oxidizing a metallic layer with an STM tip, and confirmed that the staircase period was consistent with the barrier dimension [6]. In these works, $w_{\text{dep}} \sim 0$ in metals plays a critical role. However, in semiconducting NWs, w_{dep} is large due to small n , and thus, the active NW region contributing to electron transport is much deeper in location and much narrower in radius than the actual NW size. Because of large w_{dep} , it is conceivable that two small capacitors of ~ 10 nm² \times 0.5 nm rectangular prisms can exist in NWs, in particular around the fused portion. We consider the island to be located in the fused portion and coupled to the source and drain NWs. Understanding how the source and drain NWs fuse, including

the crystal orientation of the fused portion with respect to the NWs, will be important in clarifying the physical origin and properties of the island and its surrounding potential barrier. Our I_d - V_d staircase is clear so that it would not be necessary to consider the coupling of multiple capacitors [20,21].

Since Si:H electrodes are n^+ -doped and InP NWs are unintentionally n -doped [2], and the bulk electron mobility is several ten times higher than the bulk hole mobility, we assume that only electrons contribute to transport [3]. Given characteristics of the two-probe measurement, R_{tot} reflects two different contributions, contact resistance R_c between the electrodes and NWs, and NW bulk resistance R_{NW} . Thus, $R_{\text{tot}} = R_c + R_{\text{NW}}$. In figure 5(a), R_{tot} is plotted as a function of light illumination power P . In figure 5(b), $G(P) = 1/R_{\text{tot}}(P)$ and $\Delta G(P) = G(P) - G(0)$ are plotted. We assume $R_{\text{NW}} \gg R_c$. For a cone NW, R_{NW} is given by

$$\int_0^h \rho dz / [\pi r^2(z)] = \rho h / (\pi r_i r_b) , \quad (6)$$

where ρ is the InP resistivity and $r(z)$ is the radius at height z with $r(h) = r_i$ and $r(0) = r_b$. Then, ΔG is expressed as $qA/L \times \mu \Delta n$ with the electron mobility μ , the e-h pair density Δn , the length L , and the effective cross-section $A = \pi r_i r_b$ of the NW. Without the knowledge of μ in our NWs, $\mu \Delta n$ is plotted as a function of P . Both $G(P)$ and $\Delta G(P)$ show apparent linearity. This is consistent with our starting assumption of $R_{\text{NW}} \gg R_c$. In fact, although $R_{\text{NW}} \propto 1/P$, R_c generally depends on P differently. If $R_{\text{NW}} \sim R_c$, the apparent linearity of $G(P)$ cannot be observed. The linearity suggests that $R_{\text{NW}} \gg R_c$, $R_{\text{tot}} \sim R_{\text{NW}}$, and $\Delta n \propto P$.

Now $R_{\text{NW}} = R_{\text{bulk}} + R_T$, where R_{bulk} represents the NW bulk resistance. R_{bulk} varies little while R_T changes significantly (because of exponential barrier width dependence) among different fused NW pairs. The linearity of $G(P)$ further suggests that $R_{\text{bulk}} \gg R_T$. Also, the Coulomb staircase requires isolation of the island, *i.e.*, $R_T \gg R_Q$ [13]. Thus, in dark when the clear staircase is observable, $R_{\text{bulk}} \sim 10 \text{ M}\Omega \gg R_T \gg R_Q = 12.9 \text{ k}\Omega$ for the fused NW pair dominating the photoconductor's characteristics. For the other non-dominant fused NW pairs, $R_T >$ (or \gg) $R_{\text{bulk}} \sim 10 \text{ M}\Omega$ and the resultant R_{tot} is much higher so that practically no current flows in these parallel connections. Under light illumination when the staircase disappears, $R_T \leq R_Q = 12.9 \text{ k}\Omega$ and $R_{\text{tot}} \sim R_{\text{bulk}}$ is reinforced for the dominant NW pair. In some photoconductors, the staircase was absent even in dark, and this is interpreted as C_s and C_d not small enough or $R_T \gg R_Q = 12.9 \text{ k}\Omega$ not satisfied.

Next, we will discuss how E_{F0} in dark is modulated by P in InP. When $n \sim 10^{14}$ – 10^{15} cm^{-3} , E_{F0} is located at 1.115–1.175 eV above the top of the valence band E_v ($E_g = 1.34 \text{ eV}$). Using e-h effective masses of 0.08 and 0.623, effective conduction-band and valence-band densities N_c and N_v are $5.7 \times 10^{17} \text{ cm}^{-3}$ and $1.1 \times 10^{19} \text{ cm}^{-3}$, respectively. Thus, the intrinsic carrier density n_i is $\sqrt{N_c N_v} e^{-E_g/2k_B T} = 10^7 \text{ cm}^{-3}$. P creates the same density of excess e-h pairs $\Delta n = \Delta p$. In Fig. 5(c),

$$E_{F_n} = k_B T \ln[1 + (\Delta n + n_0)/n_i] + E_{F0} , \quad (7a)$$

$$E_{F_p} = -k_B T \ln(1 + \Delta p/n_i) + E_{F0} . \quad (7b)$$

are plotted as a function of P . There is no practical difference in E_{F_n} between $n_0 = 10^{14} \text{ cm}^{-3}$ and 10^{15} cm^{-3} except for $P = 0$. The electron mobility μ was not measured and unknown. E_{F_n} and E_{F_p} were calculated for representative values, $\mu = 34.7 \text{ cm}^2/\text{Vs}$ (a theoretical lower limit for a cone-shaped NW with $n \sim 10^{15} \text{ cm}^{-3}$ [22]), $1000 \text{ cm}^2/\text{Vs}$, and $3000 \text{ cm}^2/\text{Vs}$ (an upper limit for intrinsic bulk InP). When $P = 1 \text{ }\mu\text{W}$, however, quasi-Fermi levels are fairly insensitive to μ , and $E_{F_n} \sim 1.2 \text{ eV}$ and $E_{F_p} \sim 0.30 \text{ eV}$. With further increase in P , E_{F_n} increases and E_{F_p} decreases gradually. For $P = 0$ – $5 \text{ }\mu\text{W}$, $\Delta E_{F_n} = 25$ – 85 meV . When the potential barriers are comparable to ΔE_{F_n} , the Coulomb staircase scenario should appear. The I_d - V_d curve in dark has a finite slope near $V_d = 0$ and this indicates that there was an initial "effective" charge on the Coulomb

island [5], and this gives information for the physical origin of the barriers, which we have not identified at this stage.

A similar disappearance of the Coulomb staircase was reported for an InAs NW with a pair of barriers created with InP [23]. As shown in figure 2(b) of Ref. 23, they observed the staircase disappearing with increasing gate bias. This can be interpreted in a similar way, i.e., the gate bias raised the Fermi level and a pair of potential barriers was buried resulting in the disappearance of the staircase, just like our light illumination raised the electron quasi-Fermi level and the pair of potential barriers was buried.

CONCLUSION

We have analyzed DC I_d - V_d characteristics of InP NWs between two n^+ -Si:H electrodes in dark and under light illumination. The I_d - V_d curve in dark exhibits periodic staircase steps. When the NWs are illuminated, the staircase features are suppressed and the I_d - V_d curve is Ohmic. The change is reversible by returning to dark. We have shown that everything can be explained consistently with the Coulomb staircase scenario.

- (i) InP NWs are unintentionally doped at $n \sim 10^{15} \text{ cm}^{-3}$ when the radius is significantly large, but near the NW fusion when the radius is $0.1 \text{ }\mu\text{m}$, w_{dep} is expected to be on the order of or less than $\sim 0.1 \text{ }\mu\text{m}$ with $n \sim 10^{16} \text{ cm}^{-3}$ to be consistent with the experimental observation that all devices show electrical conduction. Because of this large w_{dep} , an active conducting region is deep inside the NW, near the central axis.
- (ii) Two tunneling barriers surround a Coulomb island around the fused portion of NWs, where the NW radius and w_{dep} are comparable. The barriers are considered two series capacitors of $\sim 0.1 \text{ aF}$ and are estimated $\sim 10 \text{ nm}^2 \times 0.5 \text{ nm}$ rectangular prisms in size, which are much smaller than the fused portion due to large w_{dep} . Devices without the staircase do not have these pair of capacitors simply shows usual staircaseless I_d - V_d characteristics.
- (iii) Although there are multiple NW pairs connecting two electrodes, only one pair determines the entire electrical characteristics because R_T depends exponentially on the barrier width, and R_{tot} of a fused NW pair varies significantly from one to another.
- (iv) In dark, E_{F0} is located at $\sim 1.2 \text{ eV}$ above E_v . Under light illumination with power up to $5 \text{ }\mu\text{W}$, E_{Fh} rises by $\Delta E_{Fh} = 25\text{--}85 \text{ meV}$. The effective barrier height should be comparable to this ΔE_{Fh} .

References

- [1] Bao J, Bell D C, Capasso F, Wagner J B, Martensson T, Tragardh J and Samuelson L 2008 *Nano Lett.* **8**, 836 and references therein.
- [2] Kobayashi N P, Logeeswaran V J, Islam M S, Li X, Straznický J, Wang S Y, Williams R S and Chen Y 2007 *Appl. Phys. Lett.* **91**, 113116.
- [3] Martin T, Stanley C R, Iliadis A, Whitehouse C R and Sykes D R 1985 *Appl. Phys. Lett.* **46**, 994.
- [4] Sarkar A, Logeeswaran V J, Kobayashi N P, Straznický J, Wang S Y, Williams R S and Islam M S 277 *Proc. of SPIE* **6768**, 277.
- [5] Hanna A E and Tinkham M 1991 *Phys. Rev. B* **44**, 5919.
- [6] Matsumoto K, Ishii M, Segawa K, Oka Y, Vartanian B J and Harris J S 1996 *Appl. Phys. Lett.* **68**, 34.
- [7] Andres R P, Bein T, Dorogi M, Feng S, Henderson J I, Kubiak C P, Mahoney W, Osifchin R G and Reifengerger R 1996 *Science* **272**, 1323.
- [8] Averin D A and Likharev K K, Chap. 6 in *Mesoscopic Phenomena in Solids* ed. by Altshuler B A, Lee P A and Webb R A, (Elsevier, Amsterdam, 1991).
- [9] *Single Charge Tunneling: Coulomb Blockade Phenomena in Nanostructures*, ed. by Grabert H and Devoret M H (Plenum, New York, 1992).
- [10] Tamura H, Hasuo S and Okabe Y 1987 *J. Appl. Phys.* **62**, 3036.
- [11] Beenakker C W J 1991 *Phys. Rev. B* **44**, 1646.
- [12] Amman M, Wilkins R, Ben-Jacob E, Maker P D, and Jaklevic R C 1991 *Phys. Rev. B.* **43**, 1146.
- [13] Yamada T, Chap. 7, "Nanoelectronics Applications" in *Carbon Nanotubes: Science and Applications* ed. by Meyyappan M (CRC, Boca, Raton, 2004).
- [14] When the island is not isolated well (high tunneling probability), an electron can co-exist in the electrodes as well as the island. Then, the number of electrons on the island is not quantized.
- [15] Yamada T 2001 *Appl. Phys. Lett.* **78**, 1739.
- [16] Sloggett G J, Barton N G and Spenser S J 1986 *J. Phys. A: Math. Gen.* **19**, 2725.
- [17] Shockley W, *Electrons and holes in semiconductors, with applications to transistor electronics* (Krieger, Malabar, 1976).
- [18] Bardeen J 1947 *Phys. Rev.* **71**, 717.
- [19] In the depletion approximation, the charge distribution is approximated with a step function, but the real charge density changes smoothly with location. $w_{\text{dep}} \sim \text{radius}$ means there will be some conducting charges available deep inside the NW.
- [20] Bar-Sadeh E, Goldstein Y, Zhang C, Deng H, Abeles B and Millo O 1994 *Phys. Rev. B.* **50**, 8961.
- [21] Imamura H, Chiba J, Mitani S, Takanashi K, Takahashi S, Maekawa S and Fujimori H 2000 *Phys. Rev. B* **61**, 46.
- [22] The mobility is significantly underestimated and cannot be smaller than this value, since the surface depletion and the barriers causing the Coulomb staircase are not considered.
- [23] Thelander C, Martensson T, Bjork M T, Ohlsson B J, Larsson M W, Wallenberg L R, and Samuelson L 2003 *Appl. Phys. Lett.* **83**, 2052.

Figure captions

Figure 1. (a) Schematic of a fabricated InP nanowire (NW) photoconductor. (b) Scanning electron microscope (SEM) image (top view) of a representative InP NW photoconductor. InP NWs were selectively grown on the pair of n^+ -doped Si:H electrodes. (c) SEM image of a point where two nanowires were fused.

Figure 2. (a) I_d as a function of V_d with light power as a parameter. (b) Fourier transform of $I_d(V_d) - cV_d$, where c is a constant. The peak is at $2\pi/V = 6.6 \text{ V}^{-1}$, corresponding to the staircase period of $\Delta V = 0.95 \text{ V}$.

Figure 3. Internal energy change $\Delta(N,k) = E_N - E_k$ after incoming electron tunneling to the island from electrode k in the V_g - V_d plane. If $E_N - E_k < 0$, an electron tunnels *in* from electrode k to the island with N *final* electrons (the island electrons change from $N-1$ to N). If $E_N - E_k > 0$, an electron tunnels *out* from the island with N *initial* electrons to electrode k (the island electrons change from N to $N-1$).

Figure 4. Evolution in the number of electrons on the island for different bias V_d . (a) region A of zero current, with the number of thermodynamically allowed island electrons (N) is 0, (b) region B of unit current with $N = -1$ and 0, and (c) region C of two units of current with $N = -2, -1$, and 0. Arrows indicate how tunneling occurs and N changes.

Figure 5. (a) Resistance R_{tot} as a function of light illumination power P , where each dot represents a measured point. Inset: Schematic energy band diagrams for a Coulomb island and barriers for Fermi levels E_{F0} , E_{F1} , and E_{F2} . (b) Conductance G and $\mu\Delta n$ as a function of P . (c) E_{Fn} and E_{Fp} as a function of P for representative electron mobility μ values, 34.7 [17], 1000, and 3000 cm^2/Vs .